Macromolecules

ARTICLE

pubs.acs.org/Macromolecules

Disklike Micelles in Water from Polyethylene-Containing Diblock Copolymers

Ligeng Yin and Marc A. Hillmyer*

Department of Chemistry, University of Minnesota, 207 Pleasant St. SE, Minneapolis, Minnesota 55455-0431, United States

Supporting Information

ABSTRACT: Poly(*N*,*N*-dimethylacrylamide)−polyethylene (AE) diblock copolymers were synthesized by the combination of living anionic and reversible addition−fragmentation transfer (RAFT) polymerizations. By direct dispersion of the copolymers into water above the melting transition of polyethylene and cooling to 25 °C, disklike micelles were obtained and visualized by cryogenic transmission electron microscopy (cryo-TEM). Spherical micelles were formed from a control noncrystalline poly(*N*,*N*-dimethylacrylamide)−poly(ethylene-*alt*-propylene) (AP) sample with similar composition and overall molecular weight. In combination with differential scanning calorimetry (DSC) and wide-angle X-ray scattering (WAXS), the disklike morphology in AE micelles was ascribed to the crystallization of polyethylene, driving the formation of disklike structures in this stepwise "micellization−crystallization" protocol. Further, as evidenced by small-angle neutron scattering (SANS), chain exchange between micelles was absent at elevated temperature, and thus the crystallization upon cooling was confined within each "frozen" micelle.

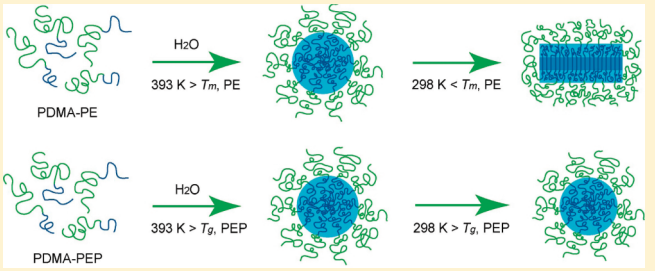

INTRODUCTION

The self-assembly of amphiphilic molecules into discrete nanostructures is of fundamental interest and has been utilized in detergency,[1] emulsion stabilization,[2,3] drug delivery,[2,3] separations,[3] and oil field[1] applications. Block copolymers offer advantages over more traditional low molecular weight lipids and surfactants in terms of enhanced stability and design flexibility that includes tailoring of the overall molecular weight, architecture, and composition.[4] Various polymers have been used as the hydrophobic micelle core.[5,6] However, perhaps due to the ease of preparation,[5] attention has focused on the rubbery or glassy materials: polybutadiene (PB),[7−11] polyisoprene (PI),[12] their saturated counterparts poly(ethylethylene) (PEE)[9] and poly(ethylene-*alt*-propylene) (PEP),[13−15] poly(propylene oxide) (PPO),[16,17] polystyrene (PS),[18−28] and polyacrylates.[29,30]

Polyethylene[31] is a material that can crystallize due to its structural regularity and offers outstanding mechanical and barrier properties.[32] Studying semicrystalline materials in micellar structures[33−46] not only provides fundamental information about core crystallization but also allows enhancement of the mechanical integrity in the nanostructures produced. Vilgis and Halperin used scaling laws to probe the micellization of coil−crystalline diblock copolymers in a coil-selective solvent and established the equilibrium parameters for disk micelles, cylinders, and large lamellae.[47] Platelet or "hockey puck"[48] structures are believed to be composed of folded crystallizable chains sandwiched by the solvated corona blocks tethered at the flat interface. Lin and Gast used self-consistent mean-field (SCF) theory in combination with a chain-folding model to account for the equilibrium structures and explored polystyrene−poly(ethylene oxide) (PS−PEO) in cyclopentane and poly(ethylene-*alt*-propylene)−polyethylene (PEP−PE) in decane as model systems.[33] The crystalline domain thickness and volume fraction profiles extracted from small-angle X-ray (SAXS) and neutron (SANS) scattering measurements were consistent with theoretical predictions. Richter et al. have also probed the platelet formation of PEP−PE in decane and found that the extended thin sheets of PE stabilized by PEP brushes were very useful as "pour point" depressants in diesel fuels.[34,49] Core crystallization also provides opportunities to trigger morphological transitions by aggregation, as shown in the formation of wormlike micelles in a triblock system with PE core[36] and superstructures from PB−PEO in heptane.[37] In water, disk micelles were observed in amphiphilic poly(2-hydroxyethyl vinyl ether) [PHOVE][50] and model collagen peptides[51] having relatively long aliphatic C18 or C20 tails, while spherical micelles formed from samples with shorter alkane groups (C12−C16). Recently, Li et al. investigated the micellization of PEO−PE diblock copolymers in water and identified various confined crystallization structures depending on sample preparation procedure.[46] These are the only two studies concerning PE-based micelles in water.

We report the synthesis of poly(*N*,*N*-dimethylacrylamide)−polyethylene (AE) diblock copolymers and characterization of their micellization behavior in water. Hydrogenated 1,4-

Received: February 2, 2011
Revised: February 22, 2011
Published: March 17, 2011

dx.doi.org/10.1021/ma200242b | *Macromolecules* 2011, 44, 3021–3028

Scheme 1. Synthetic Route toward AE and AP Diblock Copolymers

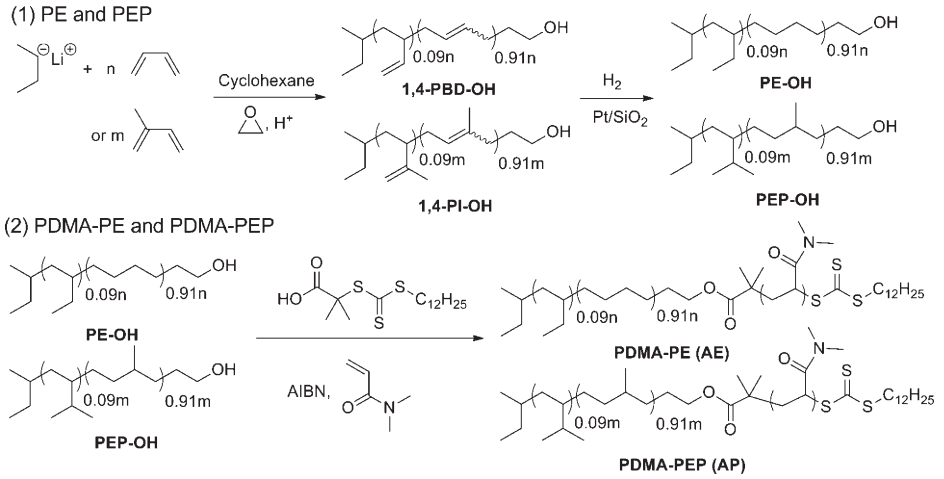

polybutadiene was chosen as a model, crystallizable linear low-density polyethylene,[32] and PDMA was chosen as the hydrophilic block due to its water solubility at elevated temperatures.[52,53] To elucidate the effect of the semicrystalline nature of the hydrophobic polyethylene block upon micellization, we also prepared noncrystalline PDMA−PEP (AP) diblock copolymers.

RESULTS

The AE and AP diblock copolymers were synthesized using a combination of anionic and reversible addition−fragmentation chain transfer (RAFT) polymerizations. As illustrated in Scheme 1, butadiene was anionically polymerized in cyclohexane and end-functionalized using ethylene oxide. Heterogeneous catalytic hydrogenation using Pt/SiO_2[54] afforded the ω-hydroxyl-functionalized PE.[55] As determined by ^{1}H NMR spectroscopy, 91% of the butadiene was incorporated in the 1,4-configuration, and full saturation (over 99%) was achieved in the hydrogenation step (Figure S1, Supporting Information). The PE homopolymer precursor is a linear low-density polyethylene (LLDPE) with 26 ethyl braches per 1000 backbone carbon atoms and a density of 0.936 g/cm^3 at 23 °C (see Experimental Section, Supporting Information).[56] An endothermic melting transition that peaked at 105 °C and a crystallinity level of 33% were determined by differential scanning calorimetry (DSC).[57] A RAFT trithiocarbonate chain transfer agent (CTA)[58] was attached to the hydroxyl end of polyethylene according to Scheme 1. The characteristic methylene proton peak neighboring the hydroxyl group in the PE precursor shifted from 3.6 to 4.1 ppm in the ^{1}H NMR spectrum (Figure S2, Supporting Information), and a new peak with the same relative intensity appeared at 3.2 ppm, corresponding to the methylene protons adjacent to the trithiocarbonate in the RAFT CTA fragment, indicating complete end-group modification. The *N*,*N*-dimethylacrylamide (DMA) monomer was then polymerized in a controlled manner to give the AE diblock copolymers with the desired length of the PDMA block.

For the AP diblocks, we followed the same protocol, except that isoprene was substituted for butadiene to give the repeating unit shown in Scheme 1. The full saturation during hydrogenation, complete end-group transformation, and successful synthesis of AP diblock copolymers were also ascertained by ^{1}H NMR spectroscopy (Figures S3 and S4, Supporting Information). For one AP sample, the blocking efficiency was further monitored using size exclusion chromatography (SEC) (as shown in Figure S5, Supporting Information). The elution curve of the diblock copolymer shifted to a lower elution volume without a detectable residual PEP homopolymer signal. In this report we focus on two samples with similar compositions and overall molecular weights, AE(9−3) and AP(11−3), and their molecular parameters are summarized in Table 1. Both of the diblocks have a relatively short hydrocarbon blocks and long water-soluble blocks that facilitate micelle preparation by direct dissolution in water.

Table 1. Molecular Characteristics of AE and AP Diblock Copolymers

sample[a]	$N_{PE(or\ PEP)}$[b]	N_{PDMA}[b]	w_{PDMA}[c]	M_n (kg/mol)[d]	PDI[e]
AE(9−3)	57	94	0.75	12	*f*
AP(11−3)	44	110	0.78	14	1.10

[a] The values in the parentheses are the number-average molecular weights in kg mol^{-1} of the component blocks, as determined by ^{1}H NMR spectroscopy. [b] Degree of polymerization. [c] Weight fraction of the PDMA block. [d] Total number-average molecular weight. [e] Determined by SEC using $CHCl_3$ as the eluent at 35 °C, relative to polystyrene standards. [f] SEC analysis of the AE sample was attempted using 1,2,4-trichlorobenzene as the eluent at 135 °C, but no detectable polymer eluted from the column, likely due to the adsorption of PDMA block.

In the preparation of the micelle samples, we directly mixed AE(9−3) with desired amount of HPLC water (0.5−3.0 wt % polymer in H_2O or H_2O/D_2O mixture) and heated the dispersion in a pressure vessel to 120 °C (i.e., above the melting transition for the PE block). The mixture became homogeneous (but not optically clear) typically after several hours and was further held at 120 °C for 5−7 days. Samples were then cooled down to 25 °C at a rate of 1−2 °C/min, and no obvious change was observed during this process. At the end of this process, typical solutions exhibited a slight blue tinge characteristic of block copolymer micellar aggregates. Micelle solutions from AP(11−3) were prepared following the same procedure.

During the course of this study we observed some hydrolysis of the PDMA block after prolonged heating at 120 °C. When held at 120 °C for 7 days, as an example, about 40% of the amide groups were hydrolyzed in AP(11−3) as determined by ^{1}H

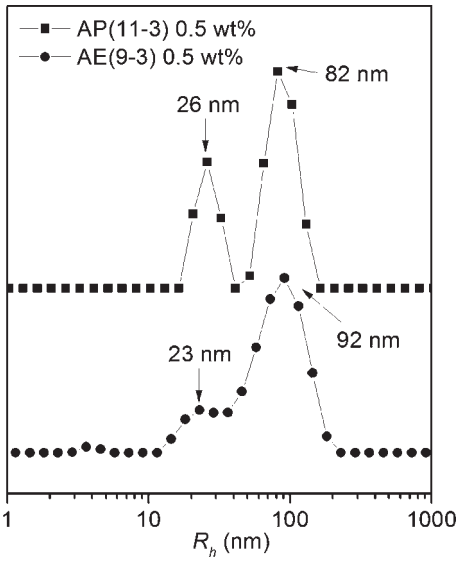

Figure 1. Apparent micelle size distributions of the AE(9−3) and AP(11−3) 0.5 wt % dispersions, generated using REPES. The scattering angle is 90°. Bimodal distributions are indicated by the two separate peaks in the distribution.

NMR spectroscopy. Hydrolysis was slowed by degassing the copolymer−water mixture prior to heating (for reasons that are unclear), although it could not be completely prevented. All samples described here were degassed and kept for about 5−7 days at the same temperature (120 °C), thus achieving a similar extent of hydrolysis. The ester linkage connecting the polyalkane and PDMA block was mostly intact after micellization (ca. 90% by end-group comparison in ^{1}H NMR spectrum, and no apparent homopolymer or separate peaks in SEC for AP(11−3); see Figure S15, Supporting Information). This can be rationalized by the fact that the micellar corona segments are highly congested at the hydrophobic interface,[59] and thus the chance of exposing the ester group directly to the aqueous media is low.

Dynamic light scattering (DLS) provides information about the average size and distribution of the micelles. The detailed sample preparation and characterization procedure can be found in the Supporting Information. The second-order scattering intensity correlation functions, $g_2(\tau)$, were measured at five different scattering angles between 60° and 120° at 25 °C and converted into the first-order correlation functions, $g_1(\tau)$, using the Siegert relation $g_2(\tau) = 1 + |g_1(\tau)|^2$. The polydispersity (defined by μ_2/Γ^2, where μ_2 is the second cumulant and Γ is the average decay rate) from the cumulant fittings of $g_1(\tau)$ was around 0.40 in both cases of AE and AP, indicating the polydisperse nature of the aggregates.[60] Moreover, two separate decay modes are present in the distribution profile generated with the REPES algorithm.[61] As such, we used a double-exponential function to fit the $g_1(\tau)$ data, and a linearity ($R^2 >$ 0.99) between the translational diffusion coefficient D and squared scattering vector q^2 was obtained for both modes. Through the Stokes−Einstein equation, two sizes of aggregates were obtained with R_h = 24, 92 nm for AE(9−3) and R_h = 25, 95 nm for AP(11−3) solutions, respectively. These values are very close to the peak positions in the distribution profile generated from the REPES algorithm, corroborating a bimodal distribution of scatterers. Furthermore, using Shibayama's proposal of bimodal (or multimodal) DLS data analysis,[62] the weight

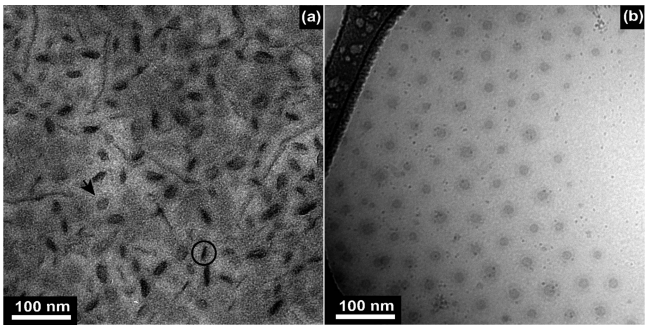

Figure 2. Representative cryo-TEM images from 0.5 wt % dispersions of (a) AE(9−3) and (b) AP(11−3), respectively. The micelle samples were made by direct dissolving the bulk samples in water and holding at 120 °C for at least 5 days, followed cooling to 25 °C before preparation for imaging. The AE(9−3) sample contains disklike micelles of "edge-on" (highlighted by black circles), "face-on" (pointed by black arrows) conformations and many others in between, while AP(11−3) contains spherical micelles as indicated by their uniformly circular cross-sections and tendency toward hexagonal packing within the thin film.

fraction of the smaller and larger aggregates in 0.5 wt % AE(9−3) solutions are estimated to be 88.6 and 11.4 wt %, respectively (89.0 and 11.0 wt % in 0.5 wt % AP(11−3) solutions). This suggests that most of the component block copolymer chains reside in the smaller aggregates. Assuming a spherical shape for both the small and large aggregates (mass $\sim R^3$), the number fraction of the smaller ones was estimated to be larger than 0.998 in both cases. This indicates that the solutions are composed of the much more populated smaller aggregates, and the probability of finding the larger ones is very low, similar to previous observations of our group.[63]

The morphology of the micelles was characterized by cryo-TEM (see Supporting Information for details), which allows direct visualization of the aggregate structures in their native aqueous environment. In the noncrystalline AP(11−3) 0.5 wt % sample, micelles with uniformly circular cross sections were observed (Figure 2b). The diffuse layer of corona is discernible in the areas proximate to the core−corona interface. These are spherical micelles, similar to previously reported micellar systems based on, for example, PEO−PB and PEO−PMCL diblock copolymers.[9,10,64] By tracking the optical density across the hydrophobic component, the micellar core radius (R_c) was determined to be 9.2 ± 1.1 nm. This corresponds to an average aggregation number of 540 (using the PEP melt density of 0.856 g/cm^3 at 25 °C[65]). The interfacial area per chain (a_0) is 2.0 nm^2. The degree of hydrophobic chain stretching (s) is 1.7, which is defined by $R_c/\langle h^2\rangle_0^{1/2}$ where $\langle h^2\rangle_0^{1/2}$ is the end-to-end distance in the random-walk configuration. These values are consistent with other highly segregated systems such as micelles from PEO−PB in water[9] or ionic liquids.[66] The R_h of the spherical micelles was estimated to be 25.7 ± 1.0 nm by taking half of the distance between the centers of two adjacent micelles as they appear to be close packed within the thin film, and this is in harmony with the size of the smaller aggregates obtained from the DLS analysis (25 nm). Consistent with the population estimation from DLS data, no large aggregates were observed in any of the grids (∼10) prepared from samples made in different trials.

In the 0.5 wt % AE(9−3) sample (Figure 2a and Figure S10, Supporting Information), the majority of the aggregates consist

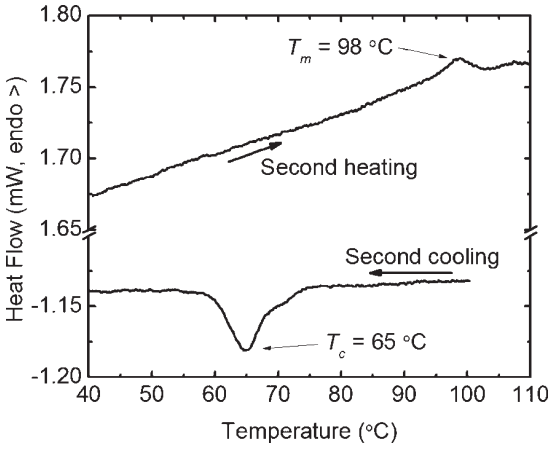

Figure 3. DSC curves of 3.0 wt % AE(9−3) micelle solutions as they were heated and cooled at a rate of 2.0 °C/min between 20 and 115 °C. Shown are the second heating and cooling scan.

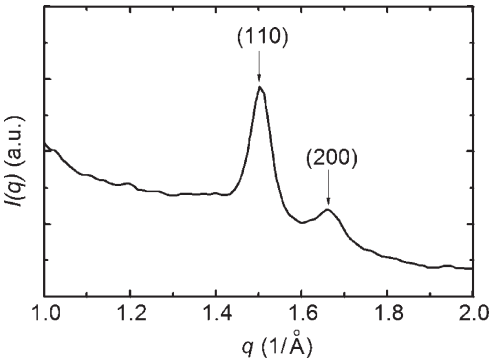

Figure 4. WAXS of 3.0 wt % AE(9−3)micelle solutions at 25 °C. Two scattering peaks were obtained in the AE(9−3) sample and can be indexed into the (110) and (200) reflections of the orthorhombic crystal lattice of polyethylene.

of small micelles; some appear much darker and have a rodlike cross section (as indicated by the black circles in Figure 2a), others have a lighter appearance and a circular cross section (indicated by the black arrows in Figure 2a), and there are structures with intermediate contrast. A small portion (less than 1% in population) of long, threadlike objects were also observed in one of the 10 grids examined. Similar micelle morphologies were observed in dispersions prepared from several other AE diblock copolymers with different compositions. The contrast mainly comes from the crystalline PE (ρ_e = 337 electrons/nm^3), since the electron density of amorphous PE (ρ_e = 313 electrons/nm^3) is very close to that of amorphous ice (ρ_e = 314 electrons/nm^3).[67] As such, the crystalline PE is most clearly visualized, while the amorphous PE and swollen PDMA corona are barely visible. We posit that these are disklike micelles, reflecting the crystalline component of the PE core. Those micelles viewed edge-on appear darker and exhibit rodlike cross sections, and those viewed face-on appear much lighter with circular cross sections, similar to the morphology of disk micelles from PEO modified lipids reported by Edwards and co-workers[68,69] and that of PE lamellar nanocrystals by Weber et al.[70] The lateral radius of the PE core crystal is estimated to be 14.3 ± 2.4 nm, and the thickness is 5.5 ± 0.8 nm. Given that the structures do appear to have some degree of kinking and are not perfectly flat disks (like a hockey puck or oblate cylinder), we refer to these micelles as disklike. The amorphous PE is expected to reside on both sides of the PE crystallites, and further surrounded by PDMA corona, as illustrated in Figure 6.

To probe the thermal behavior of these micellar assemblies, a 3.0 wt % AE(9−3) micelle solution was directly encapsulated in a hermetically sealed aluminum pan and analyzed by DSC between 20 and 115 °C. As illustrated in Figure 3, an endothermic transition peak at 98 °C was observed during the heating scan, corresponding to the melting transition of polyethylene, and an exothermic peak at 65 °C observed during the cooling scan was ascribed to be the crystallization of polyethylene. The crystallinity of the micellar cores, by tracking the second cooling scan, is determined to be ca. 30%, similar to that of the PE homopolymer precursor. In the AP(11−3) 3.0 wt % sample, no detectable thermal transitions were observed (Figure S13, Supporting Information), consistent with the rubbery nature of the micellar core.

Wide-angle X-ray scattering (WAXS) experiments were performed on the micelle solutions to extract information about the polyethylene crystal structure in the confined core of the micelles. The 3.0 wt % samples were loaded into quartz capillary tubes and exposed to the synchrotron X-ray on beamline 5 ID-D at the Advanced Photon Source of Argonne National Laboratory. As shown in Figure 4, diffraction peaks at ca. 1.50 and 1.66 Å^{-1} corresponding to the (110) and (200) reflections of the normal polyethylene orthorhombic crystal lattice were observed.[36,71] This indicates that the individual nanosized micelle cores exist in the same form as that most commonly observed in the bulk polyethylene.[32] The size of the nanocrystals were estimated to be about 25 nm from the full width at half-maximum of the (110) reflection using the Scherrer equation.[72] This is consistent with the cryo-TEM data. The AP(11−3) 3.0 wt % sample gave no detectable scattering peak (Figure S14, Supporting Information) in line with the amorphous nature of hydrophobic PEP cores.

To monitor intermicelle chain exchange, we prepared a sample with deuterated PE, A*d*E(10−3), which has similar overall molecular weight and composition to the hydrogenous AE(9−3), and used small-angle neutron scattering (SANS) and the premixing and postmixing protocol.[28,73,74] Briefly, the premixed sample was prepared by mixing the A*d*E(10−3) and AE(9−3) before being dispersed in 120 °C D_2O/H_2O mixture, whose contrast closely match that of the corona block. The postmixed samples were prepared by mixing the premade AE(9−3) and A*d*E(10−3) micelle solutions, with the postmixed−unheated one held at 25 °C, while the postmixed−heated sample was further heated at 120 °C for 1 week before the measurement at 25 °C. More details can be found in the Experimental Section of the Supporting Information. No intermicelle chain exchange is expected between the semicrystalline cores when kept at 25 °C, and thus the postmixed−unheated sample reflects the contrast condition at initial time (I_0). On the other hand, the premixed sample represents the intensity profile at long times (I_∞), if equilibration was achieved between cores with different isotopic distribution. Upon heating, if there were some chain−chain exchange between micelles, the scattering profile should be distinguished from the postmixed−unheated sample (I_0) and tends to resemble the premixed sample (I_∞). In fact, after being kept at 120 °C for 1 week, the postmixed−heated sample showed a virtually indistinguishable pattern from the unheated one, and thus the micelles are essentially "frozen" in nature even at highest temperatures accessed.

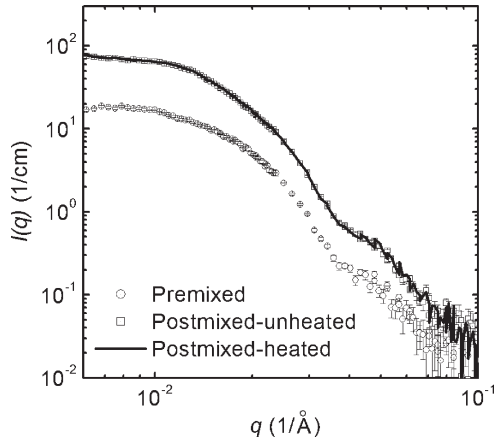

Figure 5. SANS scattering profiles obtained at 25 °C from premixed (circles), postmixed-unheated (squares), and postmixed-heated (solid line) dispersions of AE(9−3)/A*d*E(10−3) (1:1). D_2O/H_2O solvent mixtures (76:24, v/v) were used in all cases and were contrast matched with the corona PDMA block.

DISCUSSION

Now we consider the morphological differences between these two systems, namely, disklike micelles with semicrystalline PE cores and spherical micelles in the case of amorphous PEP cores. Generally, the morphology of diblock copolymer micelles can be rationalized by considering the free energy contributions from the core chains, interface, and the corona chains. In the starlike regime of coil−coil diblock copolymers, spherical micelles with highly curved interfaces are typically observed to relieve the crowding of corona chains. This is consistent with our observations for AP(11−3) micelles. Disklike micelles, on the other hand, have a relatively flat interface, and additional factors can lead to their formation. There are three different mechanisms commonly encountered in the literature of disk micelles from diblock copolymers:

(i) *Extremely strong interfacial tension.* This was implicated for disks of ∼100 nm diameter and 9 nm thickness from (nearly) symmetric polybutadiene−poly(hexafluoropropylene oxide) diblock copolymers. The disk morphology was ascribed to the extremely strong interfacial tension between the fluoropolymer core and the hydrocarbon corona leading to flat interfaces.[75]

(ii) *Rodlike corona or core blocks.* This effect was reported by Wu et al. using poly(*n*-hexyl isocyanate)−PEO in toluene, and the dominant nematic interactions between the corona rodlike blocks were suggested to drive the extended, sheetlike packing of the molecules along the interface.[76] While in the case of PEO−poly{(+)-2,5-bis[4′-((*S*)-2-methylbutoxy)phenyl]styrene} (PMBPS) dispersed in water, the formation of disklike structures was ascribed to the parallel arrangement of core PMBPS chains within the liquid crystalline domain.[77]

(iii) *Crystallization-induced morphologies.* During micelle formation, a crystallizable core block can undergo folding and regular packing, driving the development of a closely packed, lamellae-like structure. This has been shown in the cases of large platelet micelles (diameters on the order of 1 μm) from PEP−PE in decane, PS−PEO in cyclopentane,[33,34,49] and smaller disks (diameter ∼20 nm) in water from amphiphilic poly(2-hydroxyethyl vinyl ether)[50] and model collagen peptides[51] due to relatively long and crystallizable aliphatic C18 or C20 groups.

In the case of the AE(9−3) micelles, the incompatibility between the PE core and swollen PDMA corona is expected to be similar to that in the AP(11−3) spherical micelles, since both PE and PEP are hydrocarbons, thus arguing against an interfacial tension argument. There is also no reason to implicate rodlike corona blocks, as PDMA is known to form coils in water,[78] and if there is any contribution from this, we would have likely observed the effect in the AP micelles. Neither PE nor PEP is rodlike, thus arguing against the possibility of rodlike core block. Here the combined cryo-TEM, DSC, and WAXS results on the AE(9−3) and AP(11−3) micelles corroborate the mechanism of crystallization-induced formation of disklike and spherical micelles, respectively (Figure 6). When held at 120 °C, the AE(9−3) micelle solutions gave a bluish tinge to the naked eye, indicating the existence of micellar aggregates, and we speculate that the morphology of those micelles closely resembles the spherical micelles formed by AP(11−3).[79] During the process of cooling to 25 °C, the core of AP micelles remained amorphous, and no morphological transition was expected, while in the case of AE micelles, polyethylene can undergo chain-folding and regular-packing during crystallization between 75 and 55 °C, disrupting the morphology into disklike micelles due to the formation of crystalline lamellae. A similar transition was observed in amphiphilic PHOVE with hydrophobic octadecyl groups in water,[50] with the neat sample melting around 40 °C. By a combination of SAXS and SANS, Nakano et al. showed that it formed disklike micelles at room temperature and reversibly changed into spherical micelles with increasing temperature. Our work increases the number of aliphatic carbons by 1 order of magnitude, and the morphology of the aggregates formed are dictated by the thermal properties of the hydrophobic polymer, which can be simply controlled by its microstructure. PEP does not crystallize, while the confined PE described here melts around 100 °C and crystallizes between 75 and 55 °C. Furthermore, similar PE nanocrystal structures were obtained by the in situ synthesis−crystallization of PE homopolymers (stabilized by surfactants) using water-soluble Ni(II) catalysts. By choosing appropriate Ni(II) complexes, the degree of branching and crystallinity can be controlled in the homopolymers prepared.[80] Elongated structures in water were also observed in poly(ethylene-*co*-acrylic acid) (PEAA) copolymers with a modest level of carboxylic acid groups.[81]

Furthermore, we believe that the crystallization upon cooling is restricted in each individual micelle; i.e., we are probing the crystallization behavior of PE within confinement of tens of nanometers suspended in water. The dimension of PE cores reported here is 2 orders of magnitude smaller than those prepared in organic media; the diameter of the disklike structures is estimated to be about 30 nm, while that of platelet micelles from PEP−PE in decane is on the order of 1 μm.[33,34] This is due to the strong incompatibility between the aliphatic core and the aqueous media. As illustrated in Figure 6, at 120 °C, instead of being molecularly dissolved, the AE diblock copolymers self-assemble into nanosized aggregates prior to PE crystallization, as evidenced by the bluish tinge appearance of the dispersion. Furthermore, after being held at 120 °C for an extra week, the postmixed-heated sample showed virtually indistinguishable SANS profile from the unheated sample, and thus the micelles at 120 °C were also essentially "frozen" micelles; i.e., the intermicelle chain exchange was virtually prohibited.[73] In this sense, the crystallization upon cooling is believed to be confined within each micelle, and no change of the aggregation number can easily occur. And thus the disklike micelles of AE(9−3) can

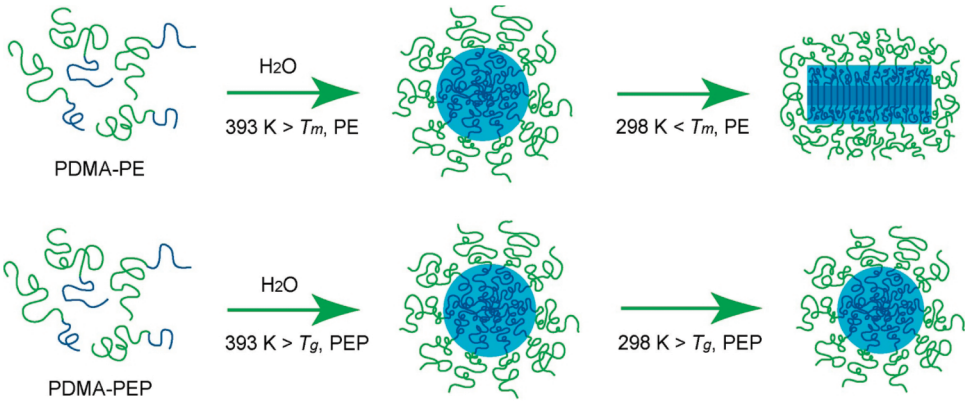

Figure 6. Hypothesized mechanism toward the formation of disklike micelles with semicrystalline PE core, and spherical micelles with rubbery PEP core, at 25 °C. The block copolymers self-assembled into spherical micelles at 120 °C, above the melting of PE or glassy transition of PEP. When cooling down to 25 °C, the crystallizable PE drove their morphology into disklike micelles, while spherical micelles remain for those with PEP cores as it was still above its glassy transition (∼−65 °C). The semicrystalline PE core is illustrated by a simplified picture of regularly packed crystalline part sandwiched by the amorphous component on both sides.

be viewed as the semicrystalline version of the spherical micelles; if no crystallization happened, the morphology of AE(9−3) micelles at 25 °C would closely resemble that of the spherical micelles from the noncrystalline AP(11−3). In the case of PEP−PE in decane, at elevated temperatures the PEP−PE copolymers were fully dissolved, and upon crystallization, each copolymer chain had sufficient molecular freedom to move to the fold interface of crystallites, thus promoting the extended, sheetlike structure up to several micrometers. Furthermore, the dimensions of PE lamellae under confinement are smaller than those in bulk PE or in PE crystallites grown from solution, whose thickness ranges from 10 to 50 nm with lateral dimension on the order of several micrometers.

CONCLUSIONS

We have reported the synthesis of an amphiphilic, polyethylene-containing diblock copolymer and investigated its micellization behavior in water. The combination of living anionic and RAFT polymerization technique allowed precise control over the length of constituent blocks. Micelle solutions were prepared by direct dissolution above the melting transition of polyethylene followed by cooling to 25 °C. Disklike micelles were obtained as evidenced by cryo-TEM visualization, in contrast to spherical micelles from a control sample with amorphous PEP core. The morphology transition was ascribed to the crystallization of polyethylene during cooling, driving the core into a close-packed, lamellae-like structure, as further supported by DSC and WAXS. Moreover, the crystallization upon cooling was believed to be confined within each "frozen" micelle, as the intermicelle chain exchange was essentially prohibited as monitored in SANS. We have demonstrated the feasibility of preparing micelles in water from semicrystalline materials in a stepwise "micellization−crystallization" manner and the impact of crystallization on the morphology disruption. The preparation of micelles of other morphologies (such as wormlike micelles) from semicrystalline PE and the enhancement of their mechanical properties are currently being explored.

ASSOCIATED CONTENT

Supporting Information. Synthesis and characterization details, ^{1}H NMR spectra and SEC traces of the precursors and block copolymers, DLS of micelle dispersions, cryo-TEM images of 0.5 wt % AE(9−3) micelle sample, DSC of bulk block copolymers, DSC and WAXS patterns of AP(11−3) 3.0 wt % micelle solutions. This material is available free of charge via the Internet at http://pubs.acs.org.

AUTHOR INFORMATION

Corresponding Author
*E-mail: hillmyer@umn.edu.

ACKNOWLEDGMENT

This work was financially supported by the Abu Dhabi−Minnesota Institute for Research Excellence (ADMIRE), a partnership between the Petroleum Institute of Abu Dhabi and the Department of Chemical Engineering and Materials Science of the University of Minnesota. Parts of this work were carried out in the Institute of Technology Characterization Facility, University of Minnesota, a member of the NSF-funded Materials Research Facilities Network. We thank Prof. Timothy P. Lodge for the discussions over the course of study and help during the SANS experiments. We also thank Dr. Liang Chen and Dr. Chun Liu for help during initial anionic polymerization and cryo-TEM imaging, respectively. Helpful discussions with Zhifeng Bai and Dr. Rajiv R. Taribagil are also gratefully acknowledged. We also acknowledge the initial efforts of Prof. Rajeswari Kasi and guidance from Prof. Frank S. Bates in the area of amphiphilic block polymers containing polyethylene.

REFERENCES

(1) Zana, R.; Kaler, E. W. *Giant Micelles: Properties and Applications*, 1st ed.; CRC Press: Boca Raton, FL, 2007.
(2) Hamley, I. W. *Block Copolymers in Solution: Fundamentals and Applications*; John Wiley & Sons, Ltd.: New York, 2005.
(3) Alexandridis, P.; Lindman, B. *Amphiphilic Block Copolymers: Self-Assembly and Applications*, 1st ed.; Elsevier: Amsterdam, 2000.
(4) Lodge, T. P.; Bang, J. A.; Li, Z. B.; Hillmyer, M. A.; Talmon, Y. *Faraday Discuss.* **2005**, *128*, 1–12.
(5) Riess, G. *Prog. Polym. Sci.* **2003**, *28* (7), 1107–1170.
(6) Gohy, J.-F. *Adv. Polym. Sci.* **2005**, *190*, 65–136.
(7) Yu, Y.; Zhang, L.; Eisenberg, A. *Langmuir* **1997**, *13* (9), 2578–2581.

(8) Won, Y.-Y.; Davis, H. T.; Bates, F. S. *Science* **1999**, *283* (5404), 960–963.
(9) Won, Y.-Y.; Brannan, A. K.; Davis, H. T.; Bates, F. S. *J. Phys. Chem. B* **2002**, *106* (13), 3354–3364.
(10) Jain, S.; Bates, F. S. *Science* **2003**, *300*, 460–464.
(11) Jain, S.; Bates, F. S. *Macromolecules* **2004**, *37* (4), 1511–1523.
(12) Bang, J.; Jain, S.; Li, Z.; Lodge, T. P.; Pedersen, J. S.; Kesselman, E.; Talmon, Y. *Macromolecules* **2006**, *39* (3), 1199–1208.
(13) Lund, R.; Willner, L.; Richter, D.; Dormidontova, E. E. *Macromolecules* **2006**, *39* (13), 4566–4575.
(14) Thompson, Z. J.; Hillmyer, M. A.; Liu, J.; Sue, H.-J.; Dettloff, M.; Bates, F. S. *Macromolecules* **2009**, *42* (7), 2333–2335.
(15) Liu, J.; Thompson, Z. J.; Sue, H.-J.; Bates, F. S.; Hillmyer, M. A.; Dettloff, M.; Jacob, G.; Verghese, N.; Pham, H. *Macromolecules* **2010**, *43* (17), 7238–7243.
(16) Schillen, K.; Bryskhe, K.; Mel'nikova, Y. S. *Macromolecules* **1999**, *32* (20), 6885–6888.
(17) Bai, Z.; Lodge, T. P. *Langmuir* **2010**, *26* (11), 8887–8892.
(18) Lifeng, Z.; Adi, E. *J. Polym. Sci., Part B: Polym. Phys.* **1999**, *37* (13), 1469–1484.
(19) Shen, H.; Zhang, L.; Eisenberg, A. *J. Am. Chem. Soc.* **1999**, *121* (12), 2728–2740.
(20) Yu, K.; Eisenberg, A. *Macromolecules* **1996**, *29* (19), 6359–6361.
(21) Yu, K.; Zhang, L.; Eisenberg, A. *Langmuir* **1996**, *12* (25), 5980–5984.
(22) Yu, Y.; Zhang, L.; Eisenberg, A. *Macromolecules* **1998**, *31* (4), 1144–1154.
(23) Zhang, L. F.; Eisenberg, A. *Science* **1995**, *268* (5218), 1728–1731.
(24) Zhu, J.; Hayward, R. C. *J. Am. Chem. Soc.* **2008**, *130* (23), 7496–7502.
(25) Chen, Q.; Zhao, H.; Ming, T.; Wang, J.; Wu, C. *J. Am. Chem. Soc.* **2009**, *131* (46), 16650–16651.
(26) Zhang, M.; Wang, M.; He, S.; Qian, J.; Saffari, A.; Lee, A.; Kumar, S.; Hassan, Y.; Guenther, A.; Scholes, G.; Winnik, M. A. *Macromolecules* **2010**, *43* (11), 5066–5074.
(27) Choi, S.-H.; Bates, F. S.; Lodge, T. P. *J. Phys. Chem. B* **2009**, *113* (42), 13840–13848.
(28) Choi, S.-H.; Lodge, T. P.; Bates, F. S. *Phys. Rev. Lett.* **2010**, *104* (4), 047802.
(29) Cui, H.; Chen, Z.; Zhong, S.; Wooley, K. L.; Pochan, D. J. *Science* **2007**, *317* (5838), 647–650.
(30) Yu, S. Y.; Azzam, T.; Rouiller, I.; Eisenberg, A. *J. Am. Chem. Soc.* **2009**, *131* (30), 10557–10566.
(31) Piringer, O. G.; Baner, A. L. *Plastic Packaging*, 2nd ed.; Wiley-VCH: Weinheim, 2008; p 32.
(32) Peacock, A. J. *Handbook of Polyethylene: Structures: Properties, and Applications*; Marcel Dekker: New York, 2000.
(33) Lin, E. K.; Gast, A. P. *Macromolecules* **1996**, *29* (12), 4432–4441.
(34) Richter, D.; Schneiders, D.; Monkenbusch, M.; Willner, L.; Fetters, L. J.; Huang, J. S.; Lin, M.; Mortensen, K.; Farago, B. *Macromolecules* **1997**, *30* (4), 1053–1068.
(35) Radulescu, A.; Mathers, R. T.; Coates, G. W.; Richter, D.; Fetters, L. J. *Macromolecules* **2004**, *37* (18), 6962–6971.
(36) Schmalz, H.; Schmelz, J.; Drechsler, M.; Yuan, J.; Walther, A.; Schweimer, K.; Mihut, A. M. *Macromolecules* **2008**, *41* (9), 3235–3242.
(37) Mihut, A. M.; Chiche, A.; Drechsler, M.; Schmalz, H.; Di Cola, E.; Krausch, G.; Ballauff, M. *Soft Matter* **2009**, *5* (1), 208–213.
(38) Massey, J. A.; Temple, K.; Cao, L.; Rharbi, Y.; Raez, J.; Winnik, M. A.; Manners, I. *J. Am. Chem. Soc.* **2000**, *122* (47), 11577–11584.
(39) Cao, L.; Manners, I.; Winnik, M. A. *Macromolecules* **2002**, *35* (22), 8258–8260.
(40) Wang, X.; Guerin, G.; Wang, H.; Wang, Y.; Manners, I.; Winnik, M. A. *Science* **2007**, *317* (5838), 644–647.
(41) Soto, A. P.; Gilroy, J. B.; Winnik, M. A.; Manners, I. *Angew. Chem., Int. Ed.* **2010**, *49* (44), 8220–8223.
(42) Ahmed, F.; Discher, D. E. *J. Controlled Release* **2004**, *96* (1), 37–53.
(43) Geng, Y.; Discher, D. E. *J. Am. Chem. Soc.* **2005**, *127* (37), 12780–12781.
(44) Rajagopal, K.; Mahmud, A.; Christian, D. A.; Pajerowski, J. D.; Brown, A. E. X.; Loverde, S. M.; Discher, D. E. *Macromolecules* **2010**, *43* (23), 9736–9746.
(45) Yin, H. Q.; Kang, S. W.; Bae, Y. H. *Macromolecules* **2009**, *42* (19), 7456–7464.
(46) Li, T.; Wang, W. J.; Liu, R.; Liang, W. H.; Zhao, G. F.; Li, Z.; Wu, Q.; Zhu, F. M. *Macromolecules* **2009**, *42* (11), 3804–3810.
(47) Vilgis, T.; Halperin, A. *Macromolecules* **1991**, *24* (8), 2090–2095.
(48) Williams, D. R. M.; Fredrickson, G. H. *Macromolecules* **1992**, *25* (13), 3561–3568.
(49) Leube, W.; Monkenbusch, M.; Schneiders, D.; Richter, D.; Adamson, D.; Fetters, L.; Dounis, P.; Lovegrove, R. *Energy Fuels* **2000**, *14* (2), 419–430.
(50) Nakano, M.; Matsumoto, K.; Matsuoka, H.; Yamaoka, H. *Macromolecules* **1999**, *32* (12), 4023–4029.
(51) Gore, T.; Dori, Y.; Talmon, Y.; Tirrell, M.; Bianco-Peled, H. *Langmuir* **2001**, *17* (17), 5352–5360.
(52) Herrera, M.; Matuschek, G.; Kettrup, A. *Chemosphere* **2001**, *42* (5−7), 601–607.
(53) Rzayev, J.; Hillmyer, M. A. *J. Am. Chem. Soc.* **2005**, *127* (38), 13373–13379.
(54) Hucul, D. A.; Hahn, S. F. *Adv. Mater.* **2000**, *12* (23), 1855–1858.
(55) Hillmyer, M. A.; Bates, F. S. *Macromolecules* **1996**, *29* (22), 6994–7002.
(56) Rosedale, J. H. Polyolefin Diblock Copolymers Near the Order-Disorder Transition. Ph.D. Thesis, Unversity of Minnesota, 1993.
(57) Mandelkern, L. *Crystallization of Polymers*; McGraw-Hill: New York, 1964.
(58) Lai, J. T.; Filla, D.; Shea, R. *Macromolecules* **2002**, *35* (18), 6754–6756.
(59) Won, Y.-Y.; Davis, H. T.; Bates, F. S.; Agamalian, M.; Wignall, G. D. *J. Phys. Chem. B* **2000**, *104* (30), 7134–7143.
(60) Chu, B. *Laser Light Scattering: Basic Principles and Practice*, 2nd ed.; Academic Press: Boston, 1991.
(61) Jakes, J. *Collect. Czech. Chem. Commun.* **1995**, *60* (11), 1781–1797.
(62) Shibayama, M.; Karino, T.; Okabe, S. *Polymer* **2006**, *47* (18), 6446–6456.
(63) Saito, N.; Liu, C.; Lodge, T. P.; Hillmyer, M. A. *Macromolecules* **2008**, *41* (22), 8815–8822.
(64) Zupancich, J. A.; Bates, F. S.; Hillmyer, M. A. *Macromolecules* **2006**, *39* (13), 4286–4288.
(65) Fetters, L. J.; Lohse, D. J.; Richter, D.; Witten, T. A.; Zirkel, A. *Macromolecules* **1994**, *27* (17), 4639–4647.
(66) He, Y. Y.; Li, Z. B.; Simone, P.; Lodge, T. P. *J. Am. Chem. Soc.* **2006**, *128* (8), 2745–2750.
(67) Using the densities from literature: 0.98 g/cm^3 (crystalline PE), 0.91 g/cm^3 (amorphous PE), and 0.94 g/cm^3 (low-density amorphous ice).
(68) Johnsson, M.; Edwards, K. *Biophys. J.* **2003**, *85* (6), 3839–3847.
(69) Sandström, M. C.; Johansson, E.; Edwards, K. *Biophys. Chem.* **2008**, *132* (2−3), 97–103.
(70) Weber, C. H. M.; Chiche, A.; Krausch, G.; Rosenfeldt, S.; Ballauff, M.; Harnau, L.; Goettker-Schnetmann, I.; Tong, Q.; Mecking, S. *Nano Lett.* **2007**, *7* (7), 2024–2029.
(71) Weimann, P. A.; Hajduk, D. A.; Chu, C.; Chaffin, K. A.; Brodil, J. C.; Bates, F. S. *J. Polym. Sci., Part B: Polym. Phys.* **1999**, *37* (16), 2053–2068.
(72) Ha, J. M.; Hamilton, B. D.; Hillmyer, M. A.; Ward, M. D. *Cryst. Growth Des.* **2009**, *9* (11), 4766–4777.
(73) Won, Y.-Y.; Davis, H. T.; Bates, F. S. *Macromolecules* **2003**, *36* (3), 953–955.
(74) Meli, L.; Santiago, J. M.; Lodge, T. P. *Macromolecules* **2010**, *43* (4), 2018–2027.

(75) Edmonds, W. F.; Li, Z.; Hillmyer, M. A.; Lodge, T. P. *Macromolecules* **2006**, *39* (13), 4526–4530.
(76) Wu, J.; Pearce, E. M.; Kwei, T. K.; Lefebvre, A. A.; Balsara, N. P. *Macromolecules* **2002**, *35* (5), 1791–1796.
(77) Zhang, H.; Lin, W. R.; Liu, A. H.; Yu, Z. N.; Wan, X. H.; Liang, D. H.; Zhou, Q. F. *Langmuir* **2008**, *24* (8), 3780–3786.
(78) Trossarelli, L.; Meirone, M. *J. Polym. Sci.* **1962**, *57*, 445–52.
(79) It is challenging in practice to quench the AE micelles prior to crystallization, though possible in principle. The structure of AE micelles at elevated temperatures can be revealed by scattering techniques (such as SANS) using appropriate sample holders, and we have those experiments planned.
(80) Tong, Q.; Krumova, M.; Gottker-Schnetmann, I.; Mecking, S. *Langmuir* **2008**, *24* (6), 2341–2347.
(81) Kryuchkov, V. A.; Daigle, J. C.; Skupov, K. M.; Claverie, J. P.; Winnik, F. M. *J. Am. Chem. Soc.* **2010**, *132* (44), 15573–15579.